

BBA 71498

## MELITTIN AND A CHEMICALLY MODIFIED TRICHOTOXIN FORM ALAMETHICIN-TYPE MULTI-STATE PORES

WOLFGANG HANKE <sup>a</sup>, CHRISTOPH METHFESSEL <sup>a</sup>, HANS-ULRICH WILMSEN <sup>a</sup>, ELLEN KATZ <sup>b</sup>, GÜNTHER JUNG <sup>b</sup> and GÜNTHER BOHEIM <sup>a,\*</sup>

<sup>a</sup> *Lehrbereich Zellphysiologie, Ruhr-Universität Bochum, Postfach 102148, D 4630 Bochum and* <sup>b</sup> *Institut für Organische Chemie, Universität Tübingen, Auf der Morgenstelle, D 7400 Tübingen (F.R.G.)*

(Received May 17th, 1982)

(Revised manuscript received August 2nd, 1982)

**Key words:** Pore formation; Alamethicin; Lipid bilayer; Ion channel; Melittin; Trichotoxin; Voltage-dependent conductance

The bee venom constituent, melittin, is structurally and functionally related to alamethicin. By forming solvent-free planar bilayers of small area (approx. 100  $\mu\text{m}^2$ ) on the tip of fire-polished glass pipettes we could observe single melittin pores in these membranes. An increase in the applied voltage induced further non-integral conductance levels. This indicates that melittin forms multi-level pores similar to those formed by alamethicin. Trichotoxin A40, an antibiotic analogue of alamethicin, also induces a voltage-dependent bilayer conductivity, but no stable pore states are resolved. However, chemical modification of the C-terminal molecule part by introduction of a dansyl group leads to a steeper voltage-dependence and pore state stabilization. Comparing structure and activity of several natural and synthetic amphiphilic polypeptides, we conclude that a lipophilic, N-terminal  $\alpha$ -helical part of adequate length (dipole moment) and a large enough hydrophilic, C-terminal region are sufficient prerequisites for voltage-dependent formation of multi-state pores.

### Introduction

The amphiphilic polypeptides alamethicin and melittin are structurally related to a large extent (Fig. 1) [1–4]. The N-terminal parts consist of lipophilic amino acids except for position [7]. A helix-breaking proline is found in position 14 and the C-termini have a quite polar character. The N-terminal regions adopt  $\alpha$ -helical conformation in organic solvents [2,3], in lipid bilayer systems [4], in aqueous solutions at high ionic strength [8] and in the crystallized state [9].  $\alpha$ -Helices bear an intrinsic dipole moment. Indeed, a dipole moment of 67 D [10] or 75 D [11], respectively, per

alamethicin molecule was found. Dipoles tend to arrange in an antiparallel fashion. At 6 Å resolution, crystallized melittin exhibits a two-fold axis of symmetry and rod-like segments which run antiparallel to each other [9,12]. Similar results were obtained for a helix-forming undecapeptide analogue of alamethicin [13]. <sup>1</sup>H-NMR spectra of the melittin tetrameric aggregate reveal proximity of isoleucine (position 2) and tryptophan (position 19), which is not observed with monomeric  $\alpha$ -helical melittin [14]. In detergent micelles, the amino-terminal and carboxy-terminal halves of the primary structure constitute separate, compact domains within the conformation of monomeric micelle-bound melittin [15,16].

Adsorption experiments with alamethicin [17] and desformyl melittin [18] at a lipid/water inter-

\* To whom correspondence should be addressed.

face reveal a large excess of monomers over oligomers. Saturation was observed at an area of approx.  $5.3 \text{ nm}^2$  per alamethicin and approx.  $6.5 \text{ nm}^2$  per desformyl melittin. The normal component of the surface dipole changed to approx. 6 D and approx. 11 D per adsorbed polypeptide, respectively. Monomer adsorption, therefore, mainly leads to tangentially oriented dipoles. This is changed to a transbilayer orientation, if an electrical field of adequate direction is applied [19]. Similarities in hemolysing properties of melittin, alamethicin and its analogues have already been shown [3,20].

It is known that aggregates of several alamethicin molecules form voltage-dependent pores in planar bilayer membranes [17,21]. A single pore exhibits a peculiar sequence of conductance levels which are not integral multiples of each other (multi-state pore) [21]. We reported that the main component of the alamethicin analogue, trichotoxin (trichotoxin A40 [5]), induced a voltage-dependent conductivity in membranes, but we failed in recording resolvable pore states [6]. Similar results were obtained by Vodyanoy et al. [22] using a purified fraction of alamethicin of unknown relation to the fraction analyzed by Melling and McMullen [23]. Here, we report that pore state conductances of trichotoxin A40 pores become resolvable after chemical modification of the C-terminal glutamyl  $\gamma$ -carboxy group by introduction of a dansyl group (Fig. 1).

Tosteson and Tosteson [24] published current fluctuations of melittin pores, which were of small conductance (7–20 pS) and long lifetime (several seconds). Evidence was presented that the melittin pores seem also to be established by molecule aggregates. We formed planar bilayer membranes of small area on the tip of fire-polished glass pipettes. This enables us to demonstrate that melittin forms multi-state pores, too.

## Materials and Methods

1-Palmitoyl-2-oleoylglycero-3-phosphocholine (1,2-POPC) and bacterial phosphatidylethanolamine (bacterial PE) were purchased 99% pure from Avanti, Birmingham, AL, U.S.A. Alamethicin F30, the carboxy-group-bearing fraction of the natural alamethicin mixture, was purchased from Micro-

bial Products Development and Production Laboratory, Porton, Salisbury, U.K.. The corresponding amide constituent alamethicin F50 was produced and purified as described elsewhere [3]. The experimental results obtained with alamethicin F30 and F50 were similar. Melittin was a gift of Dr. P. Hartter, University of Tübingen [25]. A sample of this natural mixture [1] was acetylated according to Habermann and Kowallek [26], yielding melittin derivatives with only two positive charges left at the C-terminal part.

The polypeptide antibiotic trichotoxin A is produced by the fungus *Trichoderma viride* NRRL 5242 [4]. The natural mixture was separated into two fractions, trichotoxin A40 and trichotoxin A50. Using thin-layer chromatography the components were characterized by their  $R_F$  values in the solvent system chloroform/methanol/water/acetic acid (45:35:4:3):  $R_F = 0.37$  for the A40 and  $R_F = 0.57$  for the A50. Trichotoxin A40 and A50 were highly purified by Craig counter-current distribution, and their amino acid sequences were determined [4,5]. Some natural microheterogeneity due to amino acid exchange was observed (Fig. 1). Trichotoxin A50 differs from trichotoxin A40 through exchange of glutamic acid for glutamine (position 17). Several analogues of trichotoxin A40 were obtained by chemical modification at the carboxy group (details will be published elsewhere): (1) trichotoxin A40 methyl ester ( $R_F = 0.65$ ) was prepared by addition of diazomethane in diethylether to trichotoxin A40 in anhydrous methanol. (2) Trichotoxin A40 hydrazide ( $R_F = 0.57$ ) was obtained after addition of hydrazine monohydrate to trichotoxin A40 in anhydrous methanol in a sealed vial. (3) Dansylated trichotoxin A40 ( $R_F = 0.58$ ) was obtained by reacting 5-dimethylaminonaphthalene-1-sulfochloride with trichotoxin A40 hydrazide in anhydrous methanol. The yield was approx. 95%. Furthermore, the succinyl derivative of trichotoxin A40 ( $R_F = 0.22$ ) was prepared by succinylation at the valinol hydroxy group using succinic anhydride.

Synthesis and structural analysis of the nonadecapeptide analogue (Fig. 1) have been published by Oekonomopulos and Jung [7,27]. Also synthesized was the corresponding shorter hexadecapeptide which lacks the tripeptide sequence Gly-Ala-Aib in positions 11–13 of the nonadecapeptide.

**Alamethicin F30/50**

Ac-Aib-Pro-Aib-Ala-Aib-Ala-Gln-Aib-Val-Aib-Gly-Leu-Aib-Pro-Val-Aib-Aib-Glu-Gln-Pheol  
(Aib) (Gln)

**Trichotoxin A40/50**

Ac-Aib-Gly-Aib-Leu-Aib-Gln-Aib-Aib-Aib-Ala-Aib-Aib-Pro-Leu-Aib-Iva-Glu-Valol  
(Ala) (Ala) (Aib)(Gln)

**Melittin**

For-Gly-Ile-Gly-Ala-Val-Leu-Lys-Val-Leu-Thr-Thr-Gly-Leu-Pro-Ala-Leu-Ile-Ser-Try-Ile-Lys-Arg-Lys-Arg-Gln-Gln-NH<sub>2</sub>  
(H)

**Synthetic nonadecapeptide**

Boc-Aib-Ala-Aib-Ala-Aib-Ala-Aib-Ala-Gly-Ala-Aib-Pro-Ala-Aib-Aib-Glu-Gln-OMe  
|  
Bzl

Fig. 1. Primary structures of alamethicin F30/50 [4], trichotoxin A40/50 [5,6], melittin [1] and a synthetic nonadecapeptide [7]. All polypeptides have membrane modifying properties. Abbreviations: Ac, acetyl; Aib,  $\alpha$ -aminoisobutyric acid; Boc, *tert*-butoxy-carbonyl; Bzl, benzyl; For, formyl; Iva, D-isovaline; Pheol, L-phenylalaninol; Valol, L-valinol.

Planar bilayers were formed from a solution of 2 mg lipid per ml solvent (hexane/ethanol, 9:1) on hexadecane-pretreated sandwich septa with holes approx.  $2 \cdot 10^4 \mu\text{m}^2$  in area [28]. Alternatively, lipid membranes were formed on the tip of non-pretreated fire-polished glass pipettes [29]. With the latter method, which will be presented in more detail elsewhere, seal resistances for unmodified bilayers in the gigaohm range were obtained. Whereas the tip diameter of the glass pipette was approx.  $1\text{--}2 \mu\text{m}$ , the estimate of the bilayer area on the basis of capacitance measurements yielded roughly  $100 \mu\text{m}^2$ . This indicates that the bilayers were probably located some distance inside the pipette.

The principle of the mechanical arrangement and electronic equipment is described elsewhere [21]. Current signals were recorded at a bandwidth of 3 kHz. A positive voltage is applied, if the electrical potential on the *cis*-side of the membrane is more positive than that on the *trans*-side. Positive current is directed from the *cis*- to the *trans*-side. In pipette experiments, the *trans*-side corresponds to the inside of the pipette.

**Results**

The membrane-modifying properties of alamethicin, melittin, trichotoxin A40 and several derivatives are illustrated in the following with respect to three typical features: (1) voltage-depen-

dent current-voltage characteristics (Fig. 2); (2) burst-like current fluctuations at low level of activity (Fig. 3); and (3) non-integral sequential levels of pore state conductances, if levels are resolved (Fig. 4).

**Voltage-dependent conductance**

The voltage-dependence of the polypeptide-induced bilayer conductivity is the strongest for alamethicin F30 (Fig. 2a, alamethicins F30 and F50 behave very similarly) and the weakest for melittin (Fig. 2b) and trichotoxin A40 hydrazide (Fig. 2c). Introduction of a dansyl group at the C-terminal part of trichotoxin A40 hydrazide leads to a visibly stronger voltage-dependence (Fig. 2d). In contrast to the dansylated trichotoxin A40 derivative, the others, i.e., trichotoxin A40, trichotoxin A50, trichotoxin A40 methyl ester, and succinylated trichotoxin A40, behave similarly to trichotoxin A40 hydrazide. The synthetic nonadecapeptide induces a bilayer conductivity, the voltage dependency of which is somewhat weaker than that of trichotoxin A40, whereas the synthetic hexadecapeptide is inactive.

**Low-level current fluctuations**

At low level of membrane conductivity, current fluctuations do not appear in the form of square pulse-like events of unit size as in the case of gramicidin A [30]. Sequences of events, i.e., bursts, are observed which in case of alamethicin F30

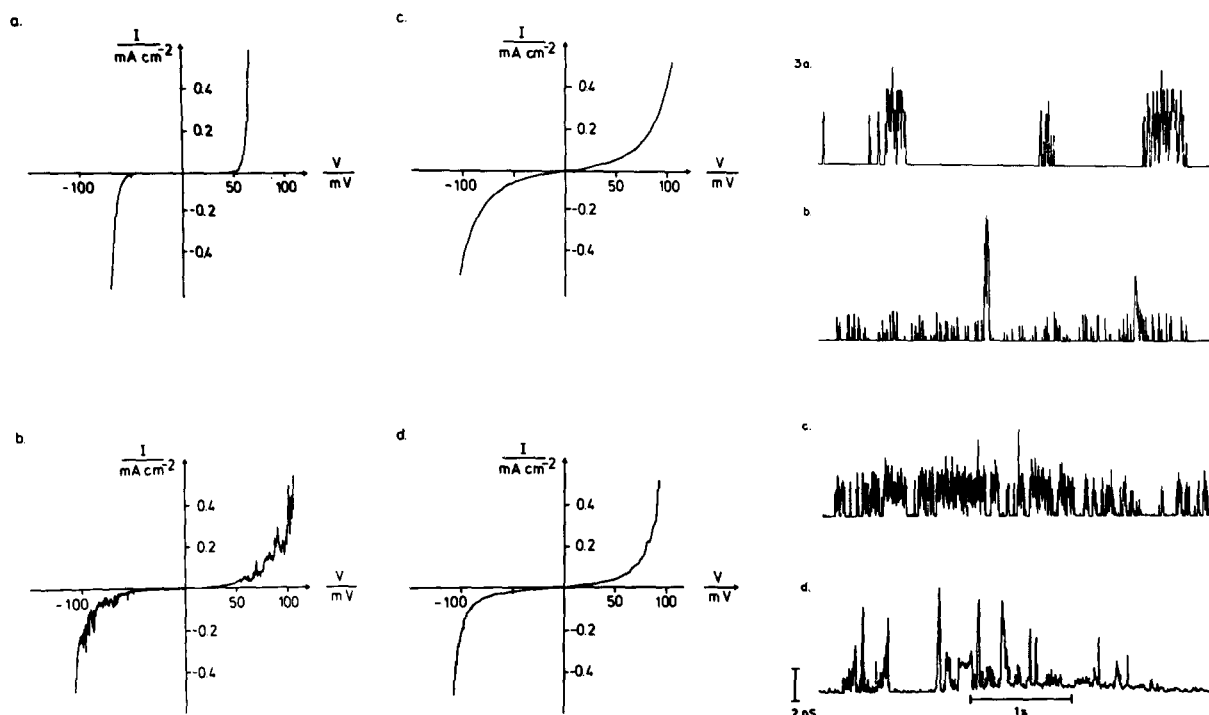


Fig. 2. Current-voltage curves of planar bilayer membranes modified by: (a) alamethicin F30; (b) melittin; (c) trichotoxin A40 hydrazide and (d) dansylated trichotoxin A40. Because of the correlation between voltage and concentration dependence of the polypeptide-induced membrane conductivity,  $\lambda$  [21], those concentrations were applied which induced  $\lambda = 1 \text{ mS} \cdot \text{cm}^{-2}$  at approx. 60–70 mV. First the positive, then the negative branch of the *I-V* curves were recorded with a voltage sweep rate of  $3 \text{ mV} \cdot \text{s}^{-1}$  in (a), (c), (d) or  $0.6 \text{ mV} \cdot \text{s}^{-1}$  in (b), respectively. The non-linear current increase is the steepest with alamethicin F30. It is steeper with dansylated trichotoxin A40 than with trichotoxin A40 hydrazide. Planar bilayers were formed from a lipid/hexane solution on a hexadecane-pretreated Teflon sandwich septum [28]. Lipid: 80% 1,2-POPC, 20% bacterial PE; salt: 1 M KCl, pH  $\approx$  6; temperature:  $20^\circ\text{C}$ ; polypeptide concentration on both sides: (a)  $0.4 \mu\text{g} \cdot \text{cm}^{-3}$  alamethicin F30; (b)  $4 \mu\text{g} \cdot \text{cm}^{-3}$  melittin; (c)  $1 \mu\text{g} \cdot \text{cm}^{-3}$  trichotoxin A40 hydrazide and (d)  $4 \mu\text{g} \cdot \text{cm}^{-3}$  dansylated trichotoxin A40.

Fig. 3. Burst-like character of membrane current fluctuations induced by (a) alamethicin, (b) acetylated melittin, (c) trichotoxin A40 and (d) dansylated trichotoxin A40. It is seen that current-changing events appear in groups (bursting). This is interpreted in case of alamethicin F30 that a pore is formed which adopts several consecutive conducting states before the pore closes [21]. Pore-state conductance levels are discernible in (a). Traces (b), (c) and (d) show the same grouping of conductance changes, but discrete conductance levels could not be resolved. This supposedly results from very short lifetimes of the pore state events. The planar bilayers were formed as described in Fig. 2 under identical conditions except for polypeptide concentrations (nominally, on *cis*-side only) and membrane voltage: (a)  $0.04 \mu\text{g} \cdot \text{cm}^{-3}$  alamethicin F30, 100 mV; (b)  $1 \mu\text{g} \cdot \text{cm}^{-3}$  acetylated melittin, 100 mV; (c)  $0.4 \mu\text{g} \cdot \text{cm}^{-3}$  trichotoxin A40, 90 mV; and (d)  $1 \mu\text{g} \cdot \text{cm}^{-3}$  dansylated trichotoxin A40, 90 mV.

(Fig. 3a) reveal transitions between discrete resolved conductance levels. A similar burst-like behaviour is observed with acetylated melittin (Fig. 3b) (the properties of which are comparable to those of the natural melittin mixture), trichotoxin A40 (Fig. 3c), dansylated trichotoxin A40 (Fig. 3d), and the synthetic nonadecapeptide (not shown). However, except for alamethicin, it is difficult to decide whether discrete conductance

levels are adopted within a burst of lifetime long enough to be resolved by our electronic measuring circuit (bandwidth limited to 3 kHz).

#### Discrete sequential pore conductance states

In order to optimize conditions for the study of discrete pore-state conductances, we altered two experimental parameters: (1) the ionic strength of the aqueous salt solution was increased to 5 M

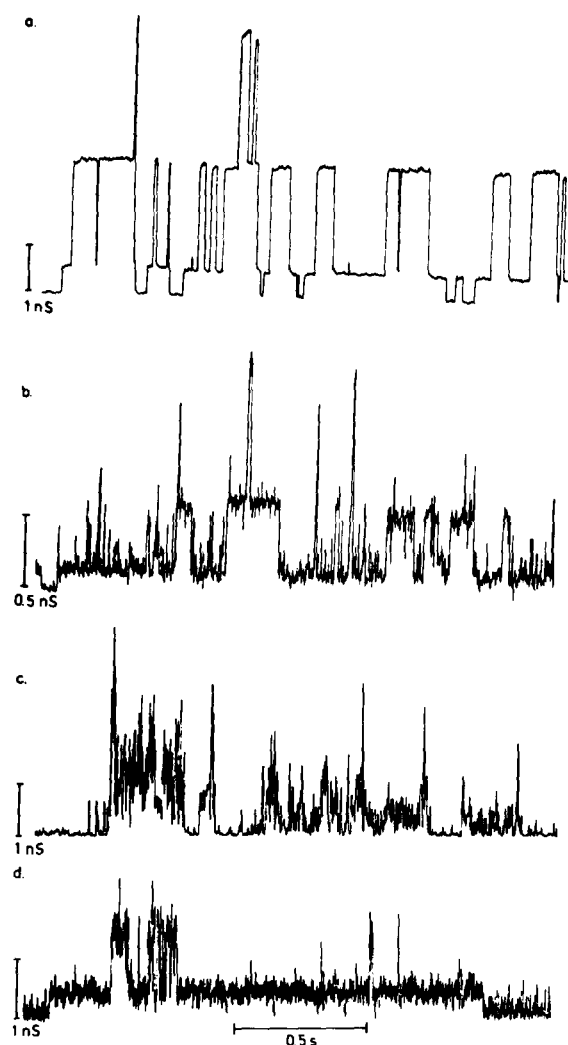


Fig. 4. Pore-state fluctuations of single pores at high ionic strength. The increase in salt concentration (5 M NaCl) and reduction of membrane area by 2 orders of magnitude (approx.  $100 \mu\text{m}^2$ ) lead to the observation of single pores with discrete resolvable conductance levels in (a) alamethicin, (b) melittin, and (d) dansylated trichotoxin A40. Only trace (c) trichotoxin A40 hydrazide, still shows unresolved current fluctuations. The peculiar feature of alamethicin-type pore fluctuations is the occurrence of consecutive conductance levels within a burst, which are not integral multiples of each other [21]. Virtually solvent-free planar bilayers were formed on the tip of non-pre-treated fire-polished glass pipettes from a lipid/hexane solution. Lipid: 1,2-POPC; salt: 5 M NaCl, pH  $\approx$  6; temperature:  $20^\circ\text{C}$ ; polypeptide concentration (nominally, in bath solution only): (a)  $0.2 \mu\text{g}\cdot\text{cm}^{-3}$  alamethicin F30, (b)  $2 \mu\text{g}\cdot\text{cm}^{-3}$  melittin (c)  $0.4 \mu\text{g}\cdot\text{cm}^{-3}$  trichotoxin A40 hydrazide (d)  $0.4 \mu\text{g}\cdot\text{cm}^{-3}$  dansylated trichotoxin A40; membrane voltage: (a,c) 100 mV, and (b,d) 110 mV.

NaCl, because enlarged pore-state lifetimes are expected; (2) membrane area was reduced by two orders of magnitude to approx.  $100 \mu\text{m}^2$ , because formation of further low-level pores is favoured over adoption of higher conductance levels of a single pore at membrane areas of at least  $1 \cdot 10^4 \mu\text{m}^2$ . Therefore, we formed virtually solvent-free planar bilayer membranes on the tip of fire-polished glass pipettes [29]. Using membranes of approx.  $100 \mu\text{m}^2$  area, we succeeded in resolving non-integral pore conductance levels in sequential order with melittin (Fig. 4b) and dansylated trichotoxin A40 (Fig. 4d). Comparison with the alamethicin F30 fluctuation trace (Fig. 4a) demonstrates that those two polypeptides form the same type of multi-level pore. In contrast, discrete pore conductance levels could not be resolved with trichotoxin A40, trichotoxin A50, trichotoxin A40 methyl ester, trichotoxin A40 hydrazide (Fig. 4c), or succinylated trichotoxin A40. The synthetic nonadecapeptide analogue is similar in behaviour to trichotoxin A40, i.e., although a voltage-dependent membrane conductivity is induced, no discrete conductance levels are resolved.

## Discussion

The experimental results presented in this paper are summarized and listed in Table I. It is seen that the bee venom constituent, melittin, forms

TABLE I

### PORE-FORMING PROPERTIES OF MEMBRANE-MODIFYING POLYPEPTIDE ANTIBIOTICS AND MELITTIN

VDC, voltage-dependent conductance; RPC, resolved pore-state conductances in 5 M NaCl.

Alamethicin F30	VDC, RPC
Alamethicin F50	VDC, RPC
Suzukacillin A [31]	VDC, RPC
Melittin	VDC, RPC
Acetylated melittin	VDC, RPC
Trichotoxin A40	VDC
Trichotoxin A40 methyl ester	VDC
Trichotoxin A40 amide	VDC
Trichotoxin A40 hydrazide	VDC
Succinylated trichotoxin A40	VDC
Dansylated trichotoxin A40	VDC, RPC
Synthetic nonadecapeptide	VDC
Synthetic hexadecapeptide	inactive

multi-level pores comparable to those formed by alamethicin. Prerequisites for voltage-dependent pore formation seem to be a large  $\alpha$ -helical part within the N-terminal region and a hydrophilic part at the C-terminal end. The positive charges on the N-terminus and the lysine residues are not essential for pore formation, as demonstrated by the experiment with an acetylated derivative. This contradicts the opinion that the positive charge of the N-terminally free glycine might function as gating charge [24]. All polypeptides tested exhibit an  $\alpha$ -helical part within the N-terminal region and induce a voltage-dependent current-voltage characteristic in planar bilayers except of the synthetic hexadecapeptide. Presumably its  $\alpha$ -helix is not large enough to span the hydrophobic membrane core. The peculiar amino acid  $\alpha$ -aminoisobutyric acid in alamethicin and its analogues is not essential for voltage-dependent pore formation. However, it shows  $\alpha$ -helix stabilizing effects [4,13,27]. Preliminary experiments with the synthetic eicosapeptide Boc-(Ala-Aib-Ala-Aib-Ala)<sub>4</sub>-OMe, which forms an ablong cylinder of  $\alpha$ -helical structure, reveal that this eicosapeptide induces a strongly voltage-dependent conductivity in planar bilayers (unpublished data). This supports the idea that this voltage-dependence originates from electrostatic interaction of the dipole moment of the  $\alpha$ -helix with the electrical field in the lipid bilayer.

A large hydrophilic C-terminus seems to stabilize the pore conductance states. Whereas the introduction of a small group ( $-\text{OCH}_3$ ,  $-\text{NH}_2$ ,  $-\text{N}_2\text{H}_3$ ) to the  $\gamma$ -carboxyl group of the C-terminal glutamic acid or the esterification of valinol with succinic anhydride does not change the voltage dependence of pore formation and the very fast pore-state fluctuations, a steeper  $I/V$  curve and resolved pore conductance levels are observed after introduction of the large dansyl group at the C-terminal molecule part. With melittin, the strong electrostatic repulsion of monomers within the pore-forming aggregate as a consequence of the positive charges (e.g., five positively charged groups in case of formylmelittin) seems to be reduced by the very large hydrophilic part and the high ionic strength. Concerning the synthetic nonadecapeptide, it is not clear as yet whether the relatively lipophilic C-terminal part or the absence of the glutamine within the N-terminal  $\alpha$ -helix causes pore-state destabilization.

The experiments described above produce strong evidence that the similarities in structure and lysing properties of alamethicin- and melittin-type peptides have a correspondence in their capability to form voltage-dependent pores. It is conceivable that the electrical field may cause orientational changes between antiparallel and parallel molecules within the peptide aggregates [13]. A series of single-pore and multi-pore experiments with trichotoxin-modified planar bilayer membranes containing decane had been published previously [32]. Single-pore current fluctuations revealed a large number of short-lived spikes superimposed on the sequence of current levels of a long-lived pore, comparable to the traces in Fig. 4b (melittin) and Fig. 4d (dansylated trichotoxin A40). As in these cases, in which the natural mixture of melittin consists of several analogues and the dansylated trichotoxin A40 contains approx. 5% of the basic compound trichotoxin A40 hydrazide, the different types of current fluctuation obtained with the first trichotoxin sample seem to reflect different pore-forming analogues. Indeed, a check of the first trichotoxin sample, with which most of the bilayer experiments were done, revealed the presence of an additional component different from trichotoxin A40 and trichotoxin A50 and from the other polypeptide antibiotics. It appears that this elusive component was produced by our *Trichoderma viride* cultures only during the first cultivation essays and had disappeared after changing to the cultivation conditions for larger antibiotic quantities. Thereafter only trichotoxin A40 and trichotoxin A50 were produced, which probably reflects a mutation in the *T. viride* strain. In view of the results presented in this paper we suggest that the short-lived spikes in the earlier work were due to trichotoxin A40 and that the long-lived pores were formed by a trichotoxin analogue of unknown structure, possibly with a larger hydrophilic C-terminus.

### Acknowledgement

We thank Dr. P. Hartter for the melittin sample. This work was supported by the Minister für Wissenschaft und Forschung des Landes Nordrhein-Westfalen (IVB4-FA8548) and the Deutsche Forschungsgemeinschaft (SFB 76, Projekt B2).

## References

- 1 Habermann, E. and Jentsch, J. (1967) Hoppe-Seyler's Z. Physiol. Chem. 348, 37–50
- 2 Habermann, E. (1972) Science 177, 314–322
- 3 Irmscher, G. and Jung, G. (1977) Eur. J. Biochem. 80, 165–174
- 4 Jung, G., Brückner, H. and Schmitt, H. (1981) in Structure and Activity of Natural Peptides (Voelter, W. and Weitzel, G., eds.), pp. 75–114, De Gruyter, Berlin
- 5 Brückner, H., König, W.A., Greiner, M. and Jung, G. (1979) Angew. Chem. Int. Edn. 18, 476–477
- 6 Jung, G., Brückner, H., Oekonomopulos, R., Boheim, G., Breitmaier, E. and König, W.A. (1979) in Peptides, Proceedings of the 6th American Peptide Symposium (Gross, E. and Meienhofer, J., eds.), pp. 647–654, Pierce Chemical Co., Rockford, IL
- 7 Oekonomopulos, R. and Jung, G. (1979) Liebigs Ann. Chem. 1979, 1151–1172
- 8 Talbot, J.C., Dufourcq, J., De Bony, J., Faucon, J.F. and Lussan, C. (1979) FEBS Lett. 102, 191–193
- 9 Terwilliger, T.C., Weissman, L. and Eisenberg, D. (1982) Biophys. J. 37, 353–361
- 10 Yantorno, R.E., Takashima, S. and Mueller, P. (1982) Biophys. J. 38, 105–110
- 11 Schwarz, G. and Savko, P. (1982) Biophys. J. 39, 211–219
- 12 Eisenberg, D., Terwilliger, T.C. and Tsui, F. (1980) Biophys. J. 32, 252–254
- 13 Butters, T., Hütter, P., Jung, G., Pauls, N., Schmitt, H., Sheldrick, G.M. and Winter, W. (1981) Angew. Chem. Int. Edn. 20, 889–890
- 14 Brown, L.R., Lauterwein, J. and Wüthrich, K. (1980) Biochim. Biophys. Acta 622, 231–244
- 15 Brown, L.R. and Wüthrich, K. (1981) Biochim. Biophys. Acta 647, 95–111
- 16 Brown, L.R., Braun, W., Kumar, A. and Wüthrich, K. (1982) Biophys. J. 37, 319–328
- 17 Gordon, L.G.M. and Haydon, D.A. (1975) Philos. Trans. R. Soc. Lond. Ser. B. 270, 433–447
- 18 Schoch, P. and Sargent, D.F. (1980) Biochim. Biophys. Acta 602, 234–247
- 19 Kempf, C., Klausner, R.D., Weinstein, J.N., Van Renswoude, J., Pincus, M. and Blumenthal, R. (1982) J. Biol. Chem. 257, 2469–2476
- 20 DeGrado, W.F., Musso, G.F., Lieber, M., Kaiser, E.T. and Kézdy, F.J. (1982) Biophys. J. 37, 329–338
- 21 Boheim, G. and Kolb, H.A. (1978) J. Membrane Biol. 38, 99–150
- 22 Vodyanoy, J., Hall, J.E., Balasubramanian, T.M. and Marshall, G.R. (1982) Biochim. Biophys. Acta 684, 53–58
- 23 Melling, J. and McMullen, A.I. (1975) SIC-IAMS Proceedings, Science Council of Japan Vol. 5, pp. 446–452
- 24 Tosteson, M.T. and Tosteson, D.C. (1981) Biophys. J. 36, 109–116
- 25 Hartter, P. and Weber, U. (1975) Hoppe Seyler's Z. Physiol. Chem. 356, 693–699
- 26 Habermann, E. and Kowallek, H. (1970) Hoppe Seyler's Z. Physiol. Chemie 351, 884–890
- 27 Oekonomopulos, R. and Jung, G. (1980) Biopolymers 19, 203–214
- 28 Schindler, H. and Feher, G. (1976) Biophys. J. 16, 1109–1113
- 29 Neher, E., Sakmann, B. and Steinbach, J.H. (1978) Pflügers Arch. 375, 219–228
- 30 Haydon, D.A. and Hladky, S.B. (1972) Q. Rev. Biophys. 5, 187–282
- 31 Boheim, G., Janko, K., Leibfritz, D., Ooka, T., König, W.A. and Jung, G. (1976) Biochim. Biophys. Acta 433, 182–199
- 32 Boheim, G., Irmscher, G. and Jung, G. (1978) Biochim. Biophys. Acta 507, 485–506